GEOLOGY | THE GEOLOGICAL SOCIETY OF AMERICA®

https://doi.org/10.1130/G50641.1

Manuscript received 3 August 2022
Revised manuscript received 10 November 2022
Manuscript accepted 20 November 2022

Published online 9 February 2023

Carbon isotope and biostratigraphic evidence for an expanded Paleocene–Eocene Thermal Maximum sedimentary record in the deep Gulf of Mexico

Lucas Vimpere[1]*, Jorge E. Spangenberg[2], Marta Roige[3], Thierry Adatte[4], Eric De Kaenel[5], Andrea Fildani[6], Julian Clark[7], Swapan Sahoo[7], Andrew Bowman[8], Pietro Sternai[9] and Sébastien Castelltort[1]

[1]Department of Earth Sciences, University of Geneva, Rue des Maraîchers 13, 1205 Geneva, Switzerland
[2]Institute of Earth Surface Dynamics (IDYST), University of Lausanne, Géopolis, 1015 Lausanne, Switzerland
[3]Departament de Geologia, Universitat Autònoma de Barcelona, 08193 Bellaterra, Spain
[4]Institute of Earth Sciences (ISTE), University of Lausanne, Géopolis, 1015 Lausanne, Switzerland
[5]DeKaenel Paleo-Research, Chemin sous la Roche 4b, 1185 Mont-sur-Rolle, Switzerland
[6]The Deep Time Institute, 23 Railroad Avenue, #804, Danville, California 94526, USA
[7]Equinor, 2107 City West Boulevard, Suite 100, Houston, Texas 77042, USA
[8]Louisiana Geological Survey, Louisiana State University 3079 Energy, Coast & Environment Building, Baton Rouge, Louisiana 70803, USA
[9]Dipartimento di Scienze dell'Ambiente e della Terra, Università degli Studi di Milano-Bicocca, Piazza della Scienza 1 e 4, I-20126 Milan, Italy

ABSTRACT

In this study, we present evidence of a Paleocene–Eocene Thermal Maximum (PETM) record within a 543-m-thick (1780 ft) deep-marine section in the Gulf of Mexico (GoM) using organic carbon stable isotopes and biostratigraphic constraints. We suggest that climate and tectonic perturbations in the upstream North American catchments can induce a substantial response in the downstream sectors of the Gulf Coastal Plain and ultimately in the GoM. This relationship is illustrated in the deep-water basin by (1) a high accommodation and deposition of a shale interval when coarse-grained terrigenous material was trapped upstream at the onset of the PETM, and (2) a considerable increase in sediment supply during the PETM, which is archived as a particularly thick sedimentary section in the deep-sea fans of the GoM basin. Despite other thick PETM sections being observed elsewhere in the world, the one described in this study links with a continental-scale paleo-drainage, which makes it of particular interest for paleoclimate and source-to-sink reconstructions.

INTRODUCTION

The Paleocene–Eocene Thermal Maximum (PETM) (ca. 56 Ma) was a rapid global warming event characterized by the rise of temperatures to 5–9 °C (Kennett and Stott, 1991), which caused substantial environmental changes around the globe. One effect was the intensification of the hydrologic cycle as a response to a changing atmospheric concentration of CO_2 (Harper et al., 2020; Rush et al., 2021). The PETM is characterized by a negative carbon isotope excursion (CIE) of roughly −3.0‰ that developed in <5 k.y. (Zeebe et al., 2016). Three main phases of the CIE have been formally identified (McInerney and Wing, 2011): (1) the "onset", defined as the time from the last samples with pre-CIE carbon isotope values to the most depleted ones; (2) the "body", which represents the interval during which isotope values were low but constant; and (3) the "recovery", during which carbon isotope values returned to pre-CIE levels.

Together with a drastic increase of the dinoflagellate cyst *Apectodinium* spp. abundance (Crouch et al., 2001) and a generalized dissolution of carbonates, it has been interpreted that large amounts of ^{13}C-depleted carbon had been released into the oceans and the atmosphere (Dickens et al., 1997). The distinctive CIE has been identified in a wide range of environments, from continental deposits to deep-water sediments (Khozyem et al., 2013), but its source is still under debate. The currently proposed hypotheses include volcanic emissions (Gutjahr et al., 2017), organic carbon from land plants and soils (Bowen, 2013) or biogenic methane (Dickens et al., 1997), or a combination of the latter two (Higgins and Schrag, 2006).

The Gulf of Mexico (GoM) is bounded by the southern coast of North America to the north, the Tampico, Vera Cruz, and Tabasco regions of Mexico to the west and south, and the Yucatán and Florida platforms to the east. It formed as a result of seafloor spreading from the Jurassic to the Early Cretaceous. From the Cretaceous to the Paleocene, mixed carbonate and clastic sediments accumulated along the northern margin of the basin (Galloway, 2008). From the late Paleocene to early Eocene, the sedimentation rate increased, resulting in a progradation of the fluvio-deltaic systems known as the Wilcox Group (Galloway and Williams, 1991). At that time, most of the southern part of North America formed a catchment area that was controlled by the contemporaneous tectonic uplift of the Laramide orogeny (Winker, 1982). The GoM then acted as the ultimate sink for the eroded material sourced from the continent (Blum and

*E-mail: lucas.vimpere@unige.ch

CITATION: Vimpere, L., et al., 2023, Carbon isotope and biostratigraphic evidence for an expanded Paleocene–Eocene Thermal Maximum sedimentary record in the deep Gulf of Mexico: Geology, v. 51, p. 334–339, https://doi.org/10.1130/G50641.1

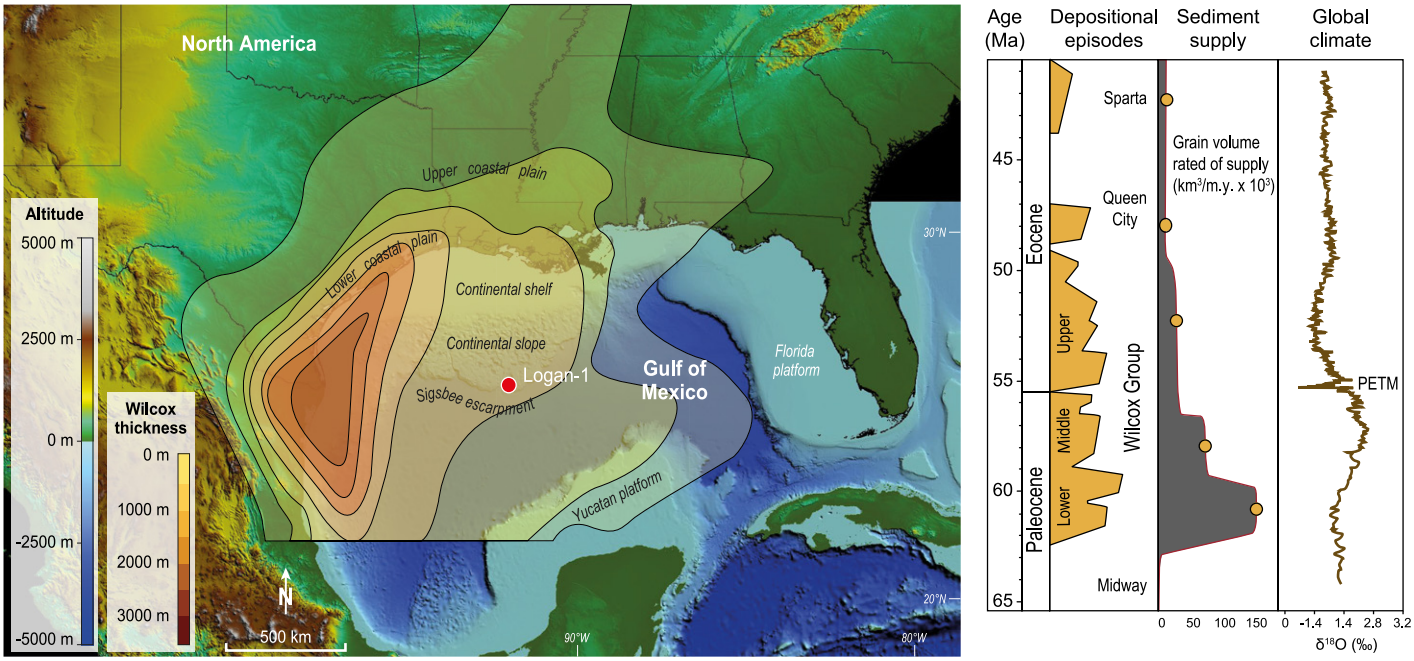

Figure 1. Topobathymetric elevation model of North America showing the Logan-1 well location (drilled in 2011 on Walker Ridge Block 969, ID WR 969 ST0 #1) and present main geographic features. Depositional context during the Paleocene-Eocene transition is represented by Wilcox Group thickness and key tectonostratigraphic events in the Gulf of Mexico sediment routing system (modified from Sharman et al., 2017). PETM—Paleocene–Eocene Thermal Maximum.

Pecha, 2014), where the deltaic systems of the Houston, Mississippi, and Rio Grande embayments funneled sediments to the deep water of the basin (Snedden and Galloway, 2019). Extensive hydrocarbon exploration has yielded a detailed stratigraphic history in the GoM. Using this framework, previous studies have identified sediment supply fluctuations throughout the Cenozoic (Galloway et al., 2011; Hessler et al., 2017; Sharman et al., 2017; Snedden et al., 2018; Zhang et al., 2018), including an increase at the end of the Paleocene (Zarra, 2007; Blum and Pecha, 2014).

The Wilcox Group comprises fluvial, deltaic, and shallow-marine facies in the outcropping sections of Texas and Alabama, shelf facies within the onshore wells drilled in the Gulf Coast, and turbidite systems in the deep-water wells (Zarra, 2007). The Wilcox Group is subdivided into the Lower, Middle, and Upper Wilcox depositional episodes (Galloway, 2008), with the Middle Wilcox being overlaid by the broad marine Yoakum Shale, which is commonly associated to the Paleocene-Eocene boundary (Galloway, 2008). Previous studies have identified the CIE associated with the PETM event in the Wilcox Group, mainly within the fluvial and deltaic deposits of North America (i.e., Bighorn Basin; Foreman et al., 2013) and of the Gulf Coastal Plain (Sluijs et al., 2014). In the distal submarine fan province of the Wilcox Group, limited data resulted in the PETM being identified from biostratigraphic data rather than from the CIE (Cunningham et al., 2022). Evidence of Cenozoic environmental changes being recorded in localized, distal deep-sea fans has revealed the propagation of the sedimentary signal across extensive sediment routing systems (thousands of kilometers), from drainages into deepest reaches of the oceans (Hessler and Fildani, 2019). When they are directly connected to a major river catchment, the high-preservation potential of deep-sea fans makes them important archives for constraining climate variations and source-to-sink dynamics (Hessler and Fildani, 2019).

We (1) identify the PETM deep-marine isotopic signal in the northern margin of the GoM basin, (2) exploit this signal as a chronostratigraphic datum in the GoM, and (3) discuss the source-to-sink dynamics of the North American sediment-routing system with respect to climate perturbations during the PETM.

MATERIAL AND METHODS

A 543-m-thick (1780 ft) section was retrieved from an ultra-deep-water wildcat well (Logan-1 well, drilled in 2011 on Walker Ridge Block 969, ID WR 969 ST0 #1) of the outboard Wilcox trend (Fig. 1), which consists of depositional lobes, locally channelized, forming part of a larger submarine fan (Fulthorpe et al., 2014). The well is located ~400 km to the southeast of New Orleans, Louisiana, in a water depth of ~2364 m and reaches a maximum depth of 8351 m below the sea surface. A total of 178 cuttings samples were collected every 3.0 m along the continuous section. Samples were prepared for bulk and clay X-ray diffraction, Rock-Eval pyrolysis, granulometric, organic carbon isotope, palynological, and calcareous nannofossil analyses (see the Supplemental Material[1]). The bulk carbon isotope composition ($\delta^{13}C_{org}$ [org—organic] values in per mil [‰] relative to Vienna Peedee belemnite [VPDB]) was determined in petroleum free cuttings (see the Supplemental Material).

EVIDENCE OF A PETM SIGNAL IN THE GULF OF MEXICO DISTAL ENVIRONMENTS

Both the palynomorphs and calcareous nannofossil bioevents identify the PETM interval between 8181 and 8001 m, with the Paleocene-Eocene boundary corresponding to the limit between the NP9 and NP10-0 horizons of calcareous nannofossil assemblages (Fig. 2; see the Supplemental Material). The CIE observed in the Logan-1 well is similar, both in terms of values and amplitude, to that described for the PETM in other wells from the U.S. margin of the GoM and other sites worldwide (Supplemental Material). The CIE (8196–8001 m) occurs 15 m below the Paleocene-Eocene boundary (Fig. 2), which supports an absence of hiatus (Khozyem et al., 2013). Similar observations

[1]Supplemental Material. Material and methods used in this study, details of the Rock-Eval, granulometric, carbon isotope, and calcareous nannofossil analyses, and correlation of the carbon isotopic curve with other sections worldwide. Please visit https://doi.org/10.1130/GEOL.S.21919362 to access the supplemental material, and contact editing@geosociety.org with any questions.

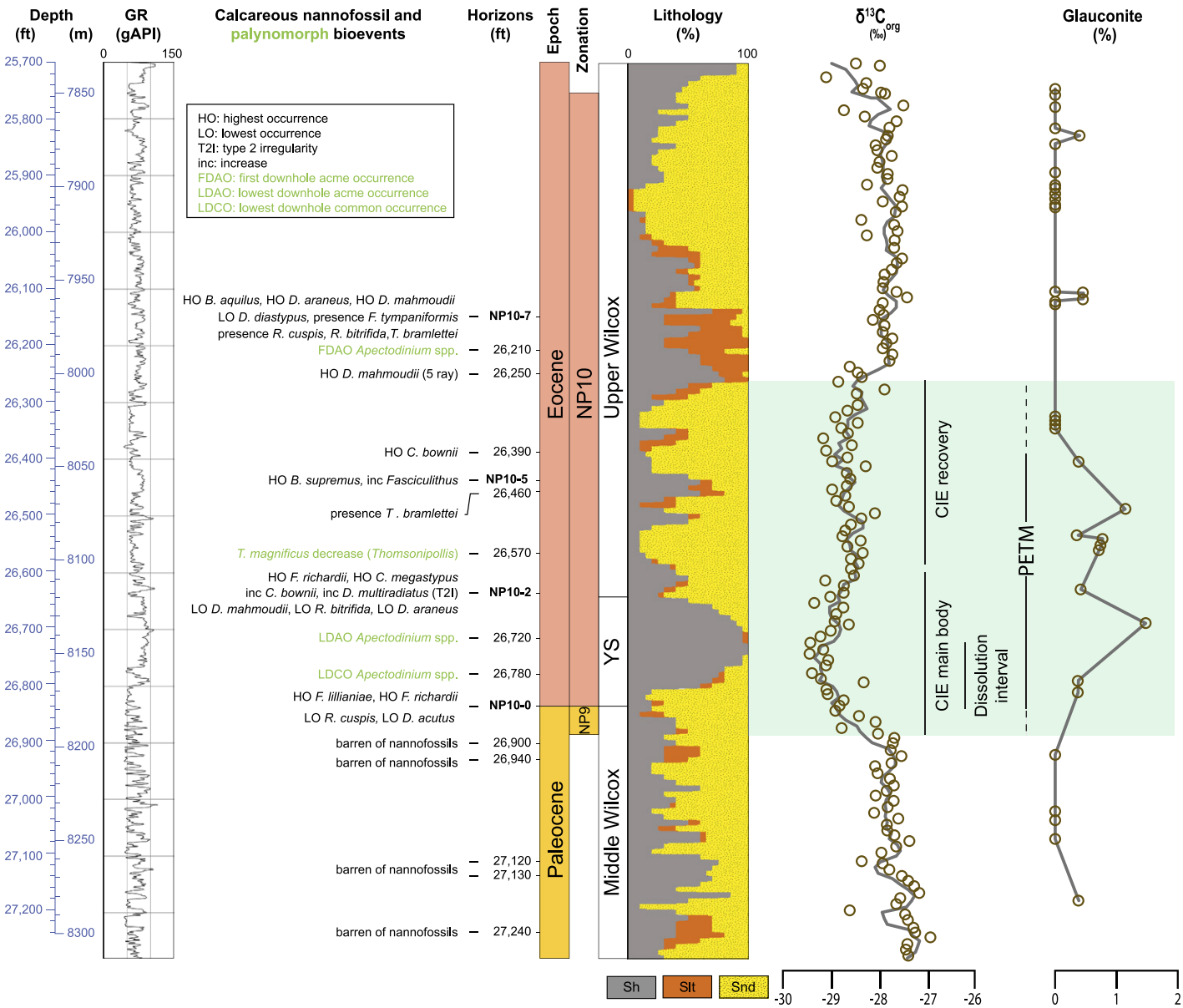

Figure 2. Carbon isotope, glauconite concentration, chronostratigraphic, and lithostratigraphic data and correlations with Gulf of Mexico standard stratigraphy for the section studied in the Logan-1 well (drilled in 2011 on Walker Ridge Block 969, ID WR 969 ST0 #1). The calcareous nannoplankton zonation is after Martini (1971). $\delta^{13}C_{org}$ measurements and three-point averages are illustrated by the circles and the curve, respectively. GR—gamma ray; Sh—shale; Slt—silt; Snd—sand; YS—Yoakum Shale; CIE—carbon isotope excursion; PETM—Paleocene–Eocene Thermal Maximum. Nannofossils: *Bomolithus aquilus*, *Discoaster araneus*, *Discoaster mahmoudii*, *Discoaster diastypus*, *Fasciculithus tympaniformis*, *Rhomboaster cuspis*, *Rhomboaster bitrifida*, *Tribrachiatus bramlettei*, *Discoaster mahmoudii*, *Coccolithus bownii*, *Bomolithus supremus*, *Tribrachiatus bramlettei*, *Thomsonipollis*, *Fasciculithus richardii*, *Caycedoae megastypus*, *Discoaster multiradiatus*, *Fasciculithus lillianiae*, *Fasciculithus richardii*, *Discoaster acutus*.

have been made elsewhere (e.g., Khozyem et al., 2015, and references therein) and correlated with the late Paleocene volcanism in the North Atlantic volcanic province, the Caribbean, and mid-ocean ridge areas (e.g., Storey et al., 2007). The CIE main body occurs between 8196 and 8108 m, and the recovery between 8108 and 8001 m, hence defining the thickest (195 m) PETM sedimentary record discovered to date. This unusual thickness contrasts with other biostratigraphically defined PETM intervals reported from several wells in the deep-water GoM basin (Cunningham et al., 2022). Identification of the PETM is further strengthened by the observed increase in the abundance of dinoflagellate cyst *Apectodinium* spp. at 8169 m (Fig. 2; see the Supplemental Material) and in glauconite concentrations at 8172 (Fig. 2; Sluijs et al., 2014). Both observations indicate a sedimentary condensation and a deposition of terrigenous material shifted landward due to a relative sea-level rise (e.g., Sluijs et al., 2014).

Our results point to significantly elevated sedimentation rates in this location of the GoM during the PETM climatic anomaly. Considering a PETM duration of 170 k.y. (Röhl et al., 2007), the overall sedimentation rate at this location was 1.15 m/k.y. The main body (88 m) and recovery (107 m) supposedly deposited over 80 and 90 k.y., respectively (Fig. 2; Röhl et al., 2007), which suggests sedimentation rates of 1.1 m/k.y. for the main body and 1.18 m/k.y. for the recovery. However, due to the difficulty

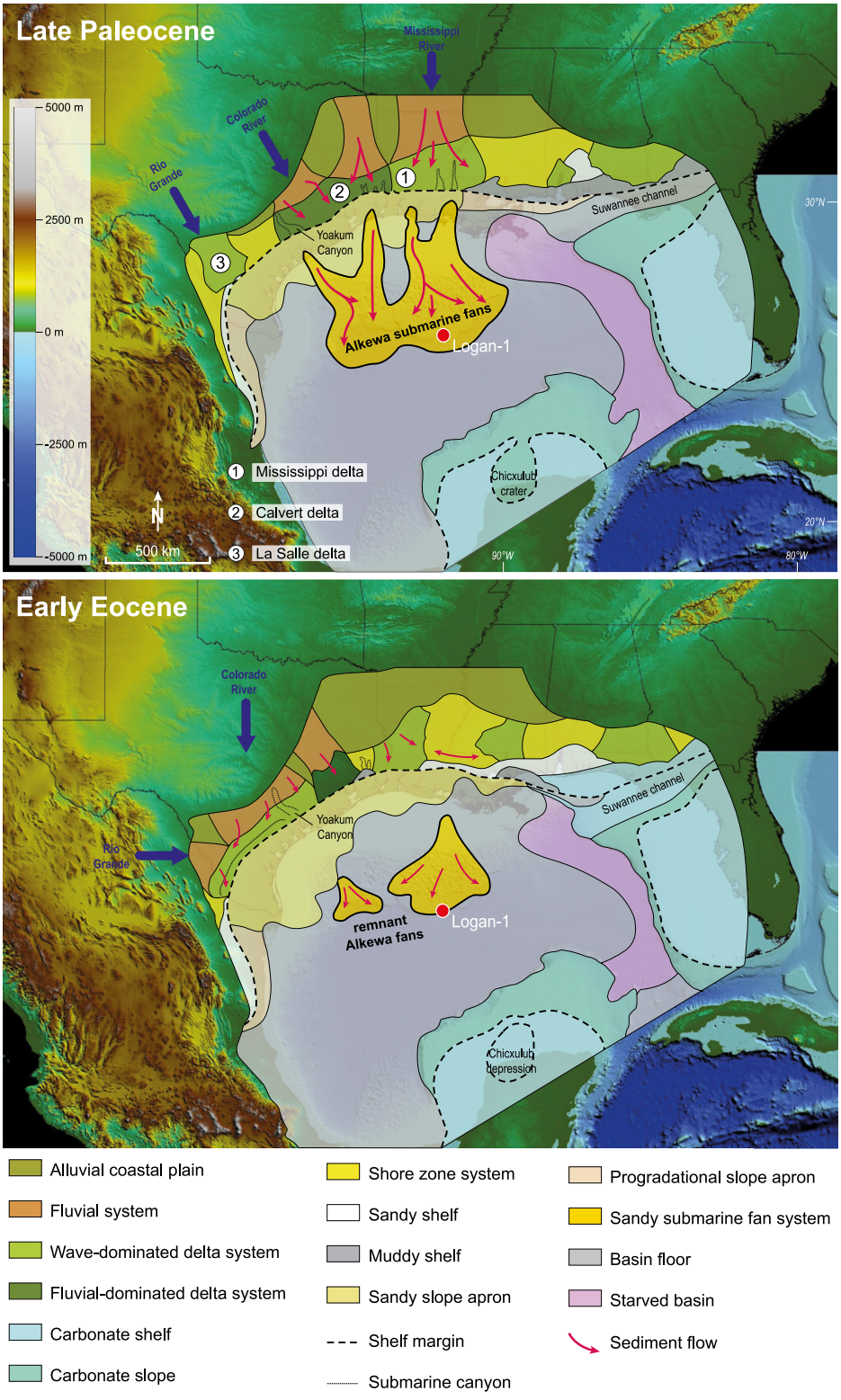

Figure 3. Paleographic map of the northern Gulf of Mexico showing evolution of the depositional systems throughout the Paleocene–Eocene Thermal Maximum (modified from Snedden and Galloway, 2019).

of distinguishing the main body from the recovery interval, substantial uncertainties surround these estimates such that the increase sedimentation rate observed for the recovery could be an artifact.

YOAKUM SHALE

The Yoakum Shale is interpreted as a maximum flooding surface, which correlates with the PETM warming and rapid transgression causing a shoreline retreat of 150 km (Galloway, 2008; Fulthorpe et al., 2014). In the Gulf Coastal Plain, it is associated with a diminished clastic supply and the formation of submarine canyons, the best known being the Yoakum Canyon in the central Texas coastal plain (Fig. 3). These canyons funneled sediments down to the basin, thus enhancing the bypass and starving of the shelf, which agrees with a higher concentration of marine palynomorphs relative to continental ones and an enrichment in glauconite observed in the proximal Sabinetown Formation outcrops in Texas and Louisiana (Galloway, 2008). The starving of the shelf and basin margin coupled with a continuous subsidence generated enough accommodation to cause, or at least to significantly contribute to, the transgression (Dingus and Galloway, 1990).

We correlate the thick glauconite-rich, clay-dominated interval presenting a CIE of 2‰ between 8175 and 8120 m with the Yoakum Shale (Fig. 2). During its deposition, climate over the continent was marked by precipitation seasonality which, coupled with a reduced vegetation cover and diminished soil moisture, ultimately increased sediment availability, channel mobility, and floodplain reworking, thus leading to a preferential transport of clays (Foreman, 2014; Barefoot et al., 2022). While coarse sediments were sequestered on the shelf, fine hemipelagic sediment continued to be transported into the deep-sea fan via turbidity currents, suspension fallout, and channeling in submarine canyons, making clays the first signal-carrying particles (Fig. 4; Hessler and Fildani, 2019). Overall, the transgression led to a concentration in the basin of the marine Yoakum Shale, which corresponds to a major flushing event that is associated with climate changes occurring over North America during the PETM.

The null hypothesis would suggest that the PETM transgression is uncoupled from sediment supply, which is to be assumed constant, but rather corresponds to a global sea-level rise (Sluijs et al., 2008). However, the proxies used record the distance from the coast rather than the magnitude of sea-level rise itself, whereas numerous studies have documented variations in sediment supply induced by climate modifications (e.g., Galloway et al., 2011). In view of this, the coupling of both mechanisms (i.e., eustasy and climate-induced variations of sediment supply) can be proposed as an alternative explanation for the observed transgression, although our data do not allow any correlation with absolute sea-level changes.

UPPER WILCOX

During the early Eocene, the drainage capture of the western U.S. rivers (Sharman et al., 2017) that followed a second pulse of Laramide uplift (Galloway et al., 2011) forced the distributary system to move toward the southwest from where sediments entered the GoM (Fig. 3). The

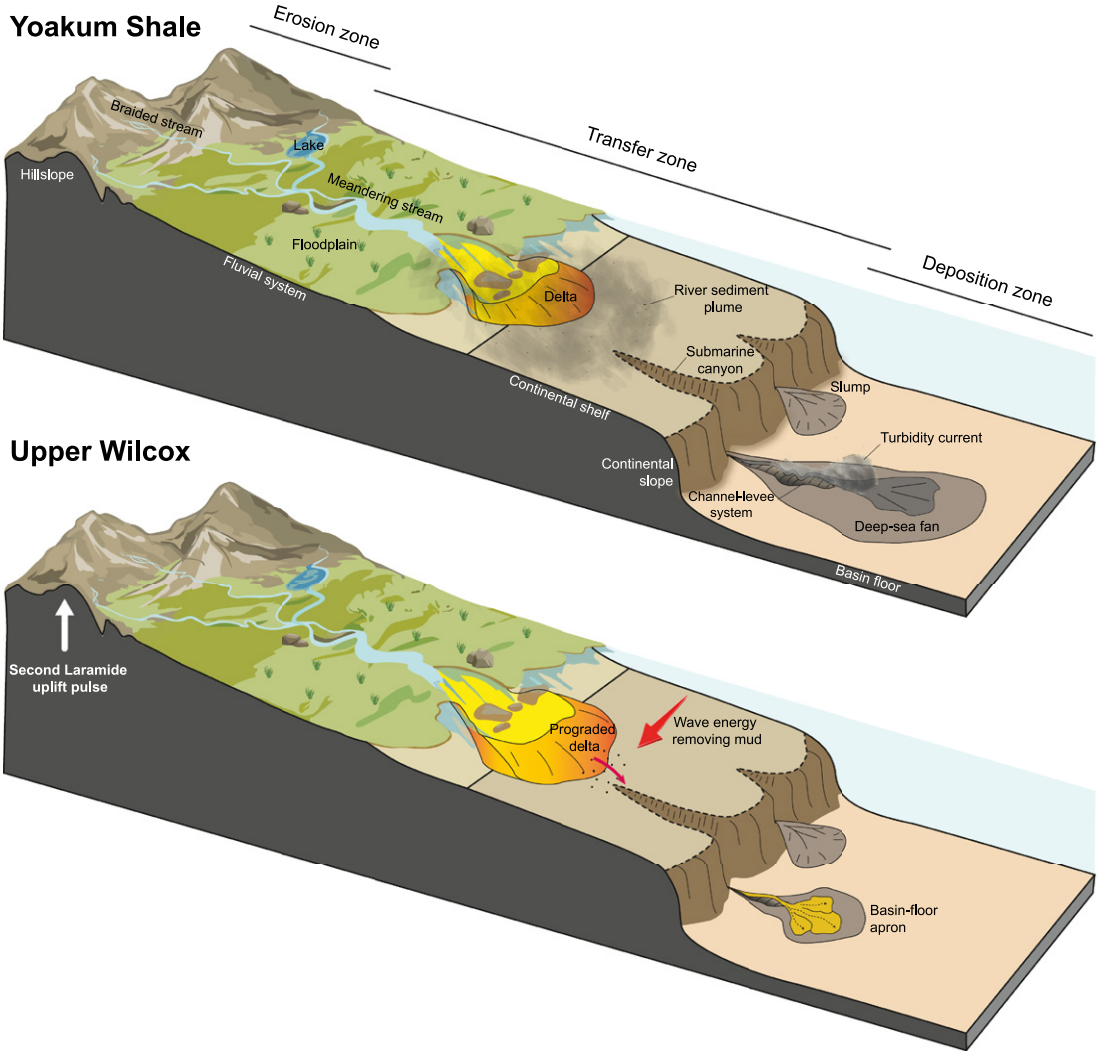

Figure 4. Schematic representation of the evolution of the sediment-routing system of North America throughout the Paleocene–Eocene Thermal Maximum. Increased channel mobility and floodplain reworking led to preferential transport of clays into the basin (i.e., Yoakum Shale) through bypass of the shelf within submarine canyons. Upper Wilcox corresponds to resuming of preferential transport of coarse material into basin-floor aprons due to progradation of deltaic sands onto the shelf and the mud removal by waves.

Upper Wilcox records the onset of the Eocene deposition through the rejuvenation of several major fluvio-deltaic systems on the coastal plain returning to equilibrium (i.e., reduced channel mobility), which ultimately supported the progradation of wave-dominated deltas to and over the shelf margin (Galloway, 2008). The progradation of coarse facies of the western deltas translates into a sandy basin-floor apron in the deep sea (Fig. 4; Fulthorpe et al., 2014), probably partly due to the sediment bypass during the initial progradation into the head of the late Paleocene canyons (e.g., Yoakum Canyon; Galloway, 2008).

The resuming of sandy turbiditic episodes and basinal apron sedimentation is represented in the Logan-1 well by the sandy beds overlying the Yoakum Shale up to 8007 m. Increase in climate extremes with more intense droughts and heavy precipitation events (Rush et al., 2021) led to sufficient runoff to create trunk streams that drained to the basin sediments derived from rocks uplifted during the late Laramide tectonic pulse (Blum and Pecha, 2014). Another mechanism could have been the concomitant wave- or current-induced removal of mud and sand transported into deep water from small wave-dominated delta lobes and sandy shore zone of the Louisiana margin (Fulthorpe et al., 2014). Either way, the observed change toward coarser sedimentation reflects the protracted transmission of catchment responses to tectonic and short-term climate perturbations down to distal systems (Foreman et al., 2012; Sharman et al., 2017).

CONCLUSIONS

Using a multi-methodological approach, we identified the Paleocene-Eocene boundary in the deep waters of the Gulf of Mexico, ~400 km away from the modern coastline. The carbon isotope ratios of organic matter reveal a pronounced CIE over a 195-m-thick section, confirmed to be the PETM excursion by the palynological and calcareous nannofossil assemblages. We demonstrate that cuttings constitute a suitable material for identifying the PETM isotopic signature when combined with sedimentary and paleontological data.

The described PETM sequence is the thickest identified by CIE, suggesting an extremely high sedimentation rate in this part of the basin. These results suggest a strong sedimentary response to changing hydrological conditions and, to a lesser extent, tectonic regimes that propagated over North America. Considering the occurrence of similar coeval fan deposits worldwide, it is reasonable to assume that extreme changes in global climate most likely influenced sedimentary routing systems during the PETM.

ACKNOWLEDGMENTS

This research was supported by Equinor, the Swiss National Science Foundation (SNSF) grant 182017 (ESSS2) to Castelltort, and the SNSF Ambizione grant 168113 to Sternai. We thank Tiffany Monnier for their valuable help in laboratory analyses. We are grateful to Eric A. Barefoot and two another anonymous reviewers for their constructive comments that helped improve the manuscript.

REFERENCES CITED

Barefoot, E.A., Nittrouer, J.A., Foreman, B.Z., Hajek, E.A., Dickens, G.R., Baisden, T., and Toms, L., 2022, Evidence for enhanced fluvial channel mobility and fine sediment export due to precipitation seasonality during the Paleocene-Eocene thermal maximum: Geology, v. 50, p. 116–120, https://doi.org/10.1130/G49149.1.

Blum, M., and Pecha, M., 2014, Mid-Cretaceous to Paleocene North American drainage reorganization from detrital zircons: Geology, v. 42, p. 607–610, https://doi.org/10.1130/G35513.1.

Bowen, G.J., 2013, Up in smoke: A role for organic carbon feedbacks in Paleogene hyperthermals: Global and Planetary Change, v. 109, p. 18–29, https://doi.org/10.1016/j.gloplacha.2013.07.001.

Crouch, E.M., Heilmann-Clausen, C., Brinkhuis, H., Morgans, H.E.G., Rogers, K.M., Egger, H., and Schmitz, B., 2001, Global dinoflagellate event associated with the late Paleocene thermal maximum: Geology, v. 29, p. 315–318, https://doi.org/10.1130/0091-7613(2001)029<0315:GDEAWT>2.0.CO;2.

Cunningham, R., Phillips, M.P., Snedden, J.W., Norton, I.O., Lowery, C.M., Virdell, J.W., Barrie, C.D., and Avery, A., 2022, Productivity and organic carbon trends through the Wilcox Group in the deep Gulf of Mexico: Evidence for ventilation during the Paleocene-Eocene Thermal Maximum: Marine and Petroleum Geology, v. 140, 105634, https://doi.org/10.1016/j.marpetgeo.2022.105634.

Dickens, G.R., Castillo, M.M., and Walker, J.C.G., 1997, A blast of gas in the latest Paleocene: Simulating first-order effects of massive dissociation of oceanic methane hydrate: Geology, v. 25, p. 259–262, https://doi.org/10.1130/0091-7613(1997)025<0259:ABOGIT>2.3.CO;2.

Dingus, W.F., and Galloway, W.E., 1990, Morphology, paleogeographic setting, and origin of the middle Wilcox Yoakum Canyon, Texas coastal plain: American Association of Petroleum Geologists Bulletin, v. 74, p. 1055–1076, https://doi.org/10.1306/0C9B2407-1710-11D7-8645000102C1865D.

Foreman, B.Z., 2014, Climate-driven generation of a fluvial sheet sand body at the Paleocene-Eocene boundary in north-west Wyoming (USA): Basin Research, v. 26, p. 225–241, https://doi.org/10.1111/bre.12027.

Foreman, B.Z., Heller, P.L., and Clementz, M.T., 2012, Fluvial response to abrupt global warming at the Palaeocene/Eocene boundary: Nature, v. 491, p. 92–95, https://doi.org/10.1038/nature11513.

Foreman, B.Z., Clementz, M.T., and Heller, P.L., 2013, Evaluation of paleoclimatic conditions east and west of the southern Canadian Cordillera in the mid-late Paleocene using bulk organic $\delta^{13}C$ records: Palaeogeography, Palaeoclimatology, Palaeoecology, v. 376, p. 103–113, https://doi.org/10.1016/j.palaeo.2013.02.023.

Fulthorpe, C.S., Galloway, W.E., Snedden, J.W., Ganey-Curry, P.E., and Whiteaker, T.L., 2014, New insights into Cenozoic depositional systems of the Gulf of Mexico Basin: Gulf Coast Association of Geological Societies Transactions, v. 64, p. 119–129.

Galloway, W.E., 2008, Depositional evolution of the Gulf of Mexico sedimentary basin, *in* Miall, A.D., ed., The Sedimentary Basins of the United States and Canada: Amsterdam, Elsevier, Sedimentary Basins of the World, v. 5, p. 505–549, https://doi.org/10.1016/S1874-5997(08)00015-4.

Galloway, W.E., and Williams, T.A., 1991, Sediment accumulation rates in time and space: Paleogene genetic stratigraphic sequences of the northwestern Gulf of Mexico basin: Geology, v. 19, p. 986–989, https://doi.org/10.1130/0091-7613(1991)019<0986:SARITA>2.3.CO;2.

Galloway, W.E., Whiteaker, T.L., and Ganey-Curry, P., 2011, History of Cenozoic North American drainage basin evolution, sediment yield, and accumulation in the Gulf of Mexico basin: Geosphere, v. 7, p. 938–973, https://doi.org/10.1130/GES00647.1.

Gutjahr, M., Ridgwell, A., Sexton, P.F., Anagnostou, E., Pearson, P.N., Pälike, H., Norris, R.D., Thomas, E., and Foster, G.L., 2017, Very large release of mostly volcanic carbon during the Palaeocene–Eocene Thermal Maximum: Nature, v. 548, p. 573–577, https://doi.org/10.1038/nature23646.

Harper, D.T., Hönisch, B., Zeebe, R.E., Shaffer, G., Haynes, L.L., Thomas, E., and Zachos, J.C., 2020, The Magnitude of surface ocean acidification and carbon release during Eocene Thermal Maximum 2 (ETM-2) and the Paleocene-Eocene Thermal Maximum (PETM): Paleoceanography and Paleoclimatology, v. 35, e2019PA003699, https://doi.org/10.1029/2019PA003699.

Hessler, A.M., and Fildani, A., 2019, Deep-sea fans: Tapping into Earth's changing landscapes: Journal of Sedimentary Research, v. 89, p. 1171–1179, https://doi.org/10.2110/jsr.2019.64.

Hessler, A.M., Zhang, J.Y., Covault, J., and Ambrose, W., 2017, Continental weathering coupled to Paleogene climate changes in North America: Geology, v. 45, p. 911–914, https://doi.org/10.1130/G39245.1.

Higgins, J.A., and Schrag, D.P., 2006, Beyond methane: Towards a theory for the Paleocene–Eocene Thermal Maximum: Earth and Planetary Science Letters, v. 245, p. 523–537, https://doi.org/10.1016/j.epsl.2006.03.009.

Kennett, J.P., and Stott, L.D., 1991, Abrupt deep-sea warming, palaeoceanographic changes and benthic extinctions at the end of the Palaeocene: Nature, v. 353, p. 225–229, https://doi.org/10.1038/353225a0.

Khozyem, H., Adatte, T., Spangenberg, J.E., Tantawy, A.A., and Keller, G., 2013, Palaeoenvironmental and climatic changes during the Palaeocene–Eocene Thermal Maximum (PETM) at the Wadi Nukhul Section, Sinai, Egypt: Journal of the Geological Society, v. 170, p. 341–352, https://doi.org/10.1144/jgs2012-046.

Khozyem, H., Adatte, T., Spangenberg, J.E., Keller, G., Tantawy, A.A., and Ulianov, A., 2015, New geochemical constraints on the Paleocene–Eocene thermal maximum: Dababiya GSSP, Egypt: Palaeogeography, Palaeoclimatology, Palaeoecology, v. 429, p. 117–135, https://doi.org/10.1016/j.palaeo.2015.04.003.

Martini, E., 1971, Standard Tertiary and Quaternary calcareous nannoplankton zonation: Proceedings of the Second Planktonic Conference, Rome, 1970, p. 739–785.

McInerney, F.A., and Wing, S.L., 2011, The Paleocene-Eocene Thermal Maximum: A perturbation of carbon cycle, climate, and biosphere with implications for the future: Annual Review of Earth and Planetary Sciences, v. 39, p. 489–516, https://doi.org/10.1146/annurev-earth-040610-133431.

Röhl, U., Westerhold, T., Bralower, T.J., and Zachos, J.C., 2007, On the duration of the Paleocene-Eocene thermal maximum (PETM): Geochemistry, Geophysics, Geosystems, v. 8, Q12002, https://doi.org/10.1029/2007GC001784.

Rush, W.D., Kiehl, J.T., Shields, C.A., and Zachos, J.C., 2021, Increased frequency of extreme precipitation events in the North Atlantic during the PETM: Observations and theory: Palaeogeography, Palaeoclimatology, Palaeoecology, v. 568, 110289, https://doi.org/10.1016/j.palaeo.2021.110289.

Sharman, G.R., Covault, J.A., Stockli, D.F., Wroblewski, A.F.-J., and Bush, M.A., 2017, Early Cenozoic drainage reorganization of the United States Western Interior–Gulf of Mexico sediment routing system: Geology, v. 45, p. 187–190, https://doi.org/10.1130/G38765.1.

Sluijs, A., et al., 2008, Eustatic variations during the Paleocene-Eocene greenhouse world: Paleoceanography, v. 23, PA4216, https://doi.org/10.1029/2008PA001615.

Sluijs, A., van Roij, L., Harrington, G.J., Schouten, S., Sessa, J.A., LeVay, L.J., Reichart, G.-J., and Slomp, C.P., 2014, Warming, euxinia and sea level rise during the Paleocene–Eocene Thermal Maximum on the Gulf Coastal Plain: Implications for ocean oxygenation and nutrient cycling: Climate of the Past, v. 10, p. 1421–1439, https://doi.org/10.5194/cp-10-1421-2014.

Snedden, J.W., and Galloway, W.E., 2019, The Gulf of Mexico Sedimentary Basin: Depositional Evolution and Petroleum Applications: Cambridge, UK, Cambridge University Press, 344 p., https://doi.org/10.1017/9781108292795.

Snedden, J.W., Tinker, L.D., and Virdell, J., 2018, Southern Gulf of Mexico Wilcox source to sink: Investigating and predicting Paleogene Wilcox reservoirs in eastern Mexico deep-water areas: American Association of Petroleum Geologists Bulletin, v. 102, p. 2045–2074, https://doi.org/10.1306/03291817263.

Storey, M., Duncan, R.A., and Swisher, C.C., 2007, Paleocene-Eocene thermal maximum and the opening of the northeast Atlantic: Science, v. 316, p. 587–589, https://doi.org/10.1126/science.1135274.

Winker, C.D., 1982, Cenozoic shelf margins: Northwestern Gulf of Mexico: Gulf Coast Association of Geological Societies Transactions, v. 32, p. 427–448.

Zarra, L., 2007, Chronostratigraphic framework for the Wilcox Formation (upper Paleocene–lower Eocene) in the deep-water Gulf of Mexico: Biostratigraphy, sequences, and depositional systems, *in* Kennan, L., et al., eds., The Paleogene of the Gulf of Mexico and Caribbean Basins: Processes, Events and Petroleum Systems: SEPM (Society for Sedimentary Geology) Gulf Coast Section SEPM Foundation 27, p. 81–145, https://doi.org/10.5724/gcs.07.27.0081.

Zeebe, R.E., Ridgwell, A., and Zachos, J.C., 2016, Anthropogenic carbon release rate unprecedented during the past 66 million years: Nature Geoscience, v. 9, p. 325–329, https://doi.org/10.1038/ngeo2681.

Zhang, J.Y., Covault, J., Pyrcz, M., Sharman, G., Carvajal, C., and Milliken, K., 2018, Quantifying sediment supply to continental margins: Application to the Paleogene Wilcox Group, Gulf of Mexico: American Association of Petroleum Geologists Bulletin, v. 102, p. 1685–1702, https://doi.org/10.1306/01081817308.

Printed in USA